AJNR

Diffusion Tensor Imaging Assessment of the Epileptogenic Zone in Children with Localization-Related Epilepsy

E. Widjaja, S. Geibprasert, H. Otsubo, O.C. Snead III and S.Z. Mahmoodabadi

This information is current as of June 4, 2024.

ORIGINAL RESEARCH

Diffusion Tensor Imaging Assessment of the Epileptogenic Zone in Children with Localization-Related Epilepsy

E. Widjaja
S. Geibprasert
H. Otsubo
O.C. Snead III
S.Z. Mahmoodabadi

BACKGROUND AND PURPOSE: Patients with MR imaging-negative epilepsy could have subtle FCD. Our aim was to determine if structural changes could be identified by using DTI in children with intractable epilepsy, from MR imaging-visible FCD and MR imaging-negative localization-related epilepsy, that were concordant with the epileptogenic zone as defined by using the MEG dipole cluster.

MATERIALS AND METHODS: Eight children with MR imaging-visible FCD and 16 with MR imaging-negative epilepsy underwent DTI and MEG. Twenty-six age-matched healthy children underwent DTI. Analysis was performed on controls across individual patients. Agreement between the location of DTI abnormalities and FCD and MEG dipole clusters was assessed.

RESULTS: In patients with MR imaging-visible FCD, abnormal FA, MD, λ_1, λ_2, and λ_3 were lobar concordant with the MEG dipole cluster in 4/8 (50.0%), 5/8 (62.5%), 3/8 (37.5%), 6/8 (75.0%), and 5/8 (62.5%), respectively. In patients with MR imaging-visible FCD, abnormal FA, MD, λ_1, λ_2, and λ_3 overlapped the x-, y-, and z-axes of the MEG dipole cluster in 1/8 (12.5%), 4/8 (50%), 4/8 (50%), 6/8 (75%), and 4/8 (50%), respectively, and with FCD in 1/8 (12.5%), 3/8 (37.5%), 0/8 (0%), 3/8 (37.5%), and 1/8 (12.5%), respectively. In patients with MR imaging-negative epilepsy, abnormal FA, MD, λ_1, λ_2, and λ_3 were lobar-concordant with the MEG dipole cluster in 11/16 (68.8%), 11/16 (68.8%), 8/16 (50.0%), 10/16 (62.5%), and 10/16 (62.5%), respectively, and overlapped the x-, y-, and z-axes of the MEG dipole cluster in 9/16 (56.3%), 10/16 (62.5%), 8/16 (50%), 8/16 (50%), and 8/16 (50%), respectively. There was no significant difference between abnormal DTI lobar concordance with the MEG dipole cluster in patients with MR imaging-visible FCD and MR imaging-negative epilepsy.

CONCLUSIONS: White matter changes can be detected with DTI in children with MR imaging-visible FCD and MR imaging-negative epilepsy, which were concordant with the epileptogenic zone in more than half of the patients.

ABBREVIATIONS: EEG = electroencephalography; FA = fractional anisotropy; FCD = focal cortical dysplasia; FLE = frontal lobe epilepsy; FMRIB = Functional MR Imaging of the Brain Library; λ_1, λ_2, and λ_3 = eigenvalues; MD = mean diffusivity; MEG = magnetoencephalography; MNI = Montreal Neurological Institute; SPM = statistical parametric mapping; TBSS = tract-based spatial statistics; TLE = temporal lobe epilepsy; VBM = voxel-based morphometry

Approximately 30%–40% of those with focal seizures are medically resistant.[1-3] In a selected subpopulation of these children, surgical treatment may be the only option to achieve a seizure-free outcome.[4-6] A lesion can be detected with MR imaging in 30%–85% of patients with refractory localization-related epilepsy.[7,8] Some of the patients with MR imaging-negative localization-related epilepsy have subtle FCD that is not readily identifiable on routine MR imaging. Up to 72% of patients with MR imaging-negative epilepsy who had surgery were found to have FCD, and others have nonspecific findings such as gliosis on histopathology.[9-13] Identification of an anatomic abnormality has important therapeutic and prognostic implications, with considerably better outcomes in patients with an identifiable lesion than in those with MR imaging-negative localization-related epilepsy.[14] Therefore, alternative imaging techniques are required to improve detection of subtle structural changes.

The white matter adjacent to FCD frequently disclosed subtle abnormalities, such as gliosis, gray matter heterotopia with abnormal neurons, and abnormal myelination on histology.[15-18] DTI is a sensitive tool to identify microstructural changes in the white matter. Three studies addressed the use of DTI in MR imaging-negative localization-related epilepsy by using voxel-based SPM[19] in adult patients, and the results were variable.[20-22] Abnormal MD has been found in 26.7%–86.7%, and abnormal FA has been identified in 6.7%–42.9% of patients with MR imaging-negative epilepsy.[20-22]

There are currently no data on DTI in children with MR imaging-negative localization-related epilepsy. Chronic recurrent seizures could result in white matter injury.[23] Given the shorter duration of epilepsy in children compared with adults, it is not known whether white matter changes can be identified by using DTI in the pediatric population with MR imaging-negative localization-related epilepsy. Our aim was to determine if structural changes could be identified by using DTI in children with intractable localization-related epilepsy

PEDIATRICS

ORIGINAL RESEARCH

from MR imaging-visible FCD and MR imaging-negative epilepsy that were concordant with the epileptogenic zone, as defined by using the MEG dipole cluster.

Materials and Methods
This study was approved by the institutional research ethics board.

Subjects
Twenty-four consecutive patients with MR imaging-visible FCD or MR imaging-negative localization-related epilepsy, consisting of 16 females and 8 males, mean age of 12.0 years (range, 5.1–18.5 years), who were being evaluated for epilepsy surgery were recruited. Clinical data, including age at seizure onset, mean duration of epilepsy, invasive intracranial monitoring, and surgical outcomes, are reported in On-line Table 1. All patients had localization-related epilepsy as determined by ictal video EEG and MEG. Eight children had MR imaging-visible FCD, and 16 children had MR imaging-negative localization-related epilepsy. Twenty-six age-matched healthy controls, 12 females and 14 males, without neurologic or psychiatric disorders and normal MR imaging findings, were included. Healthy controls were recruited through posters and Web-based publications requesting healthy children to volunteer for a research study at the Hospital for Sick Children. The mean age of the controls was 11.5 years (range, 5.1–18 years).

MR Imaging and DTI
MR imaging and DTI were performed on a 3T scanner (Achieva, Philips Healthcare, Best, the Netherlands) by using an 8-channel phased array head coil in patients and controls. Anatomic imaging consisted of axial and coronal FLAIR (TR/TE = 1000/140 ms, section thickness = 3 mm, FOV = 22 cm, matrix = 316 × 290), T2 and proton-density (TR/TE = 4200/80/40 ms, section thickness = 3 mm, FOV = 22 cm, matrix = 400 × 272), and sagittal 3D T1 (TR/TE = 4.9/2.3 ms, section thickness = 1 mm, FOV = 22 cm, matrix = 220 × 220). DTI was acquired by using single-shot diffusion-weighted echo-planar imaging, b=1000 s/mm^2 and 15 noncollinear directions (TR/TE = 10,000/60 ms, section thickness = 2 mm, FOV = 22 cm, matrix = 112 × 112, NEX = 2, sensitivity-encoding factor = 2).

DTI Image Analysis
Image analysis was performed on a group of controls across individual patients. Images were processed off-line by using FSL (FMRIB Centre, University of Oxford, Oxford United Kingdom; www.fmrib.ox.ac.uk/fsl). Correction for eddy-current induced distortions was performed.[24] Subsequently, the diffusion tensor was calculated,[25] and FA, MD, and eigenvalue (λ_1, λ_2, and λ_3) maps were generated by using DTIFit in FSL. Voxelwise statistical analysis of FA data was performed by using TBSS implemented in FSL.[26]

FA images were preprocessed and brain-extracted by using the Brain Extraction Tool.[26,27] One representative control, 11 years of age, was selected and linearly registered to the MNI152 template by using the linear image-registration tool routine of FMRIB. All FA images were linearly registered to the representative case, followed by nonlinear registration by using the nonlinear image registration tool of FMRIB. The transformed FA images were then averaged to create a mean FA image, which was then thinned so that the FA skeleton represented the center of all tracts common to the group. This was thresholded to FA ≥0.20 to include the major white matter pathways but exclude peripheral tracts where there was significant intersubject variability and/or partial volume effects with gray matter. Each subject's aligned FA data were then projected onto the skeleton. Voxelwise differences in projected FA between each patient and all the controls were tested by using a randomization procedure with 500 permutations with the threshold-free cluster enhancement option to avoid the initial cluster-forming threshold. This tool used a permutation-based statistical inference that did not rely on the Gaussian model[28] and was suited for nonstandard statistics or when the noise distribution was unknown. The resulting statistical maps were superimposed on the FA image. All the processing performed for FA was used to analyze MD and the 3 eigenvalues. Subsequently voxelwise statistical analysis was performed, and the resulting statistical maps were superimposed on MD and eigenvalue images.

MEG
MEG was performed in patients by using a whole-head Omega 151-channel gradiometer system (VSM MedTech, Port Coquitalam, British Columbia, Canada). MEG acquisition and analysis have previously been described.[29] MEG spike sources were classified into 2 groups[30]: A cluster was defined as a group of ≥6 spike sources with ≤1 cm between adjacent sources; scatters consisted of groups of either <6 spike sources, regardless of the distance between the spike sources, or groups of spike sources with >1 cm between each spike source, regardless of the number of spike sources in the group. MEG dipole clusters have previously been shown to correspond to the epileptogenic zone.[31]

MEG dipoles that had been coregistered to volumetric T1 imaging were linearly and nonlinearly registered to the MNI152 T1 template. The resulting FA, MD, and eigenvalue statistical maps were then overlaid onto the registered MEG images and visually assessed by 2 pediatric neuroradiologists independently. The findings were categorized as lobar-concordant if >50% of the DTI abnormality was located in the same lobe as the MEG dipole cluster, irrespective of whether there were unilateral or bilateral DTI changes. They were nonconcordant if >50% of the DTI abnormality was located in different lobes of the same hemisphere or in the hemisphere contralateral to the MEG dipole cluster or was of equal distribution in both hemispheres; they were negative if there was no DTI abnormality detected. The maximum transverse, anteroposterior, and craniocaudal margins of the MR imaging-visible abnormality; the MEG dipole cluster; and abnormal FA, MD, λ_1, λ_2, and λ_3 were defined on the x-, y-, and z-axes of MNI coordinates in those with MR imaging-visible FCD and MR imaging-negative epilepsy. If several areas of abnormal DTI were present, these areas were considered as 1 conglomerate area and the x-, y-, and z-axes distributions of the abnormal DTI were defined as the largest transverse, anteroposterior, and craniocaudal extent of the abnormal conglomerate area. Agreement among MR imaging-visible FCD, the MEG dipole cluster, and abnormal DTI was defined as overlap in all 3 x-, y-, and z-axes. DTI lobar concordance with the MEG dipole cluster was compared between those with MR imaging-visible FCD and MR imaging-negative epilepsy by using the χ^2 test in the Statistical Package for the Social Sciences, Version 15 (SPSS, Chicago, Illinois).

Results

Invasive Monitoring and Surgery
Eleven patients (5 with MR imaging-visible FCD and 6 with MR imaging-negative localization-related epilepsy) underwent invasive monitoring; video EEG and MEG dipole clusters in these patients were concordant with an invasive monitor-
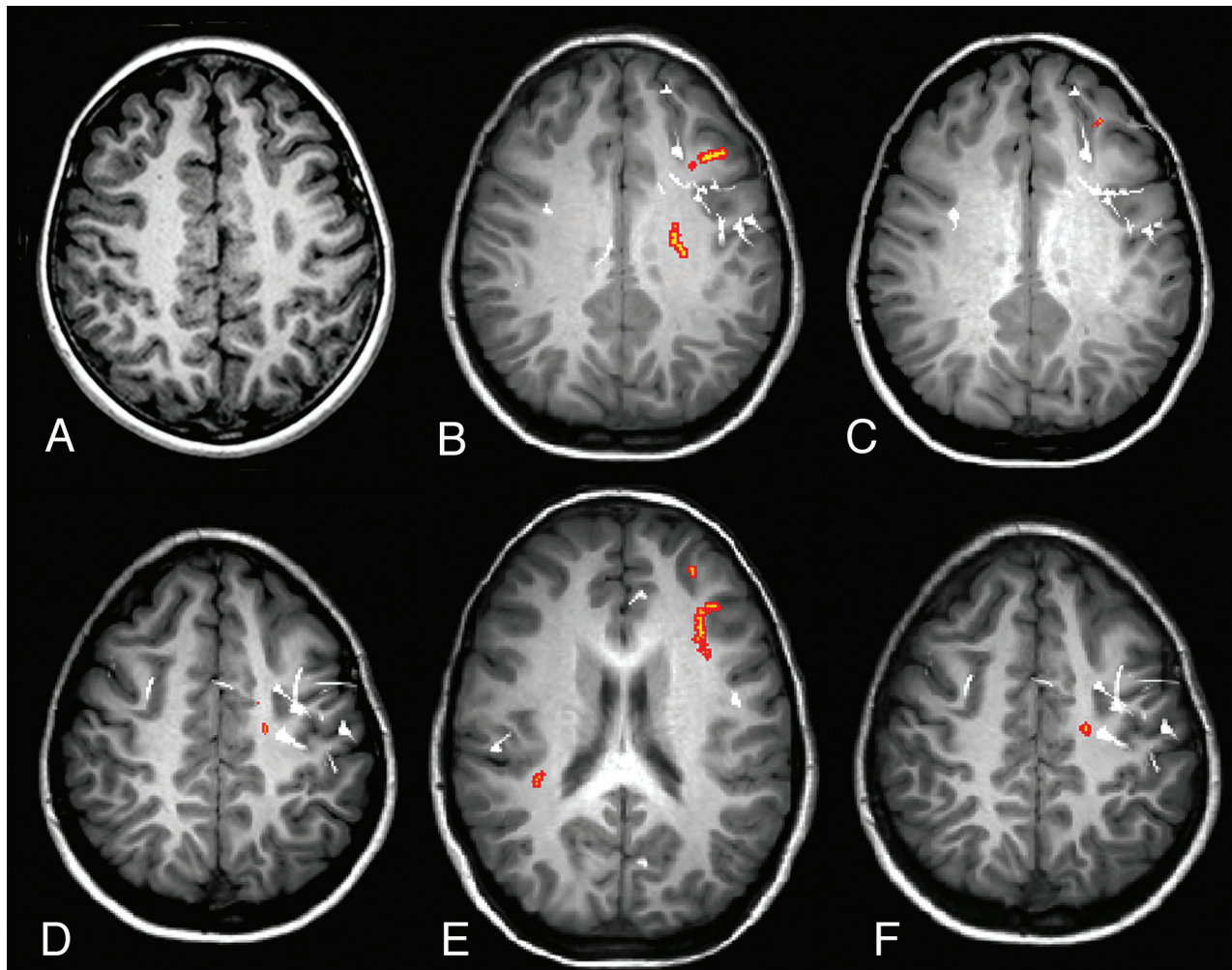
Fig 1. Case 19. *A*, Axial volumetric T1-weighted image demonstrates thickening of the cortex in the left frontal gyrus (*arrow*), associated with blurring of gray-white matter, in keeping with FCD. Regions with abnormal FA (*B*), MD (*C*), λ1 (*D*), λ_2 (*E*), and λ_3 (orange areas) (*F*) and MEG dipoles (white) are overlaid onto volumetric T1-weighted image. The MEG dipole cluster, corresponding to the epileptogenic zone, is localized to the left frontal lobe and a few scattered dipoles in the right frontal lobe. There is lobar concordance of abnormal FA, MD, and eigenvalues with the MEG dipole cluster. There are bilateral abnormal λ_2s, most of which are localized to the left frontal lobe. There is also overlap among the x-, y-, and z-axes distributions of abnormal FA, MD, and 3 eigenvalues with the MEG dipole cluster.

ing-defined epileptogenic zone. Nine patients underwent surgical resection, and 2 did not proceed to resection because the epileptogenic zone involved the motor cortex (On-line Table 1). Two patients had anterior temporal lobe resection without invasive monitoring because the MR imaging-visible FCD, video EEG, and MEG dipole cluster were concordant and localized to the left temporal lobe.

Patients with MR Imaging-Visible FCD
There was no interobserver variability with respect to lobar concordance of DTI abnormalities, MR imaging-visible FCD, and MEG dipole cluster.

Abnormal FA was identified in 8/8 (100%) and was lobar-concordant to the MEG dipole cluster in 4/8 (50%) (Fig 1). The x-, y-, and z-axes distributions of the FCD, MEG dipole cluster, and abnormal FA are shown in On-line Table 2. One (12.5%) case showed overlap between the distributions of FA abnormality and the MEG dipole cluster, and 1/8 (12.5%) showed overlap between FA abnormality and MR imaging-visible FCD in all 3 x-, y-, and z-axes.

Abnormal MD was identified in 7/8 (87.5%) and was lo-

bar-concordant to the MEG dipole cluster in 5/8 (62.5%), lobar discordant to the MEG dipole cluster in 2/8 (25.0%), and negative in 1/8 (12.5%). Four (50%) cases showed overlap between the distributions of the MD abnormality and the MEG dipole cluster in all 3 x-, y-, and z-axes, and 3/8 (37.5%) showed overlap between the distributions of MD abnormality and MR imaging-visible FCD in all 3 axes.

All 8 cases demonstrated abnormalities in all 3 eigenvalues. Lobar concordance to the MEG dipole cluster was present in 3/8 (37.5%) with λ_1 abnormality, 6/8 (75%) with λ_2 abnormality, and 5/8 (62.5%) with λ_3 abnormality. Four (50%) cases showed overlap between the distribution of the λ_1 abnormality and the MEG dipole cluster, and none of the cases demonstrated overlap between the λ_1 abnormality and MR imaging-visible FCD in all 3 x-, y-, and z-axes. Six (75%) cases showed overlap between the distribution of the λ_2 abnormality with the MEG dipole cluster, and 3/8 (37.5%) cases demonstrated overlap between the λ_2 abnormality and the MR imaging-visible FCD in all 3 x-, y-, and z-axes. In 4/8 (50%) cases, there was overlap between the distribution of the λ_3 abnormality and the MEG dipole cluster, and 1/8 (12.5%) had
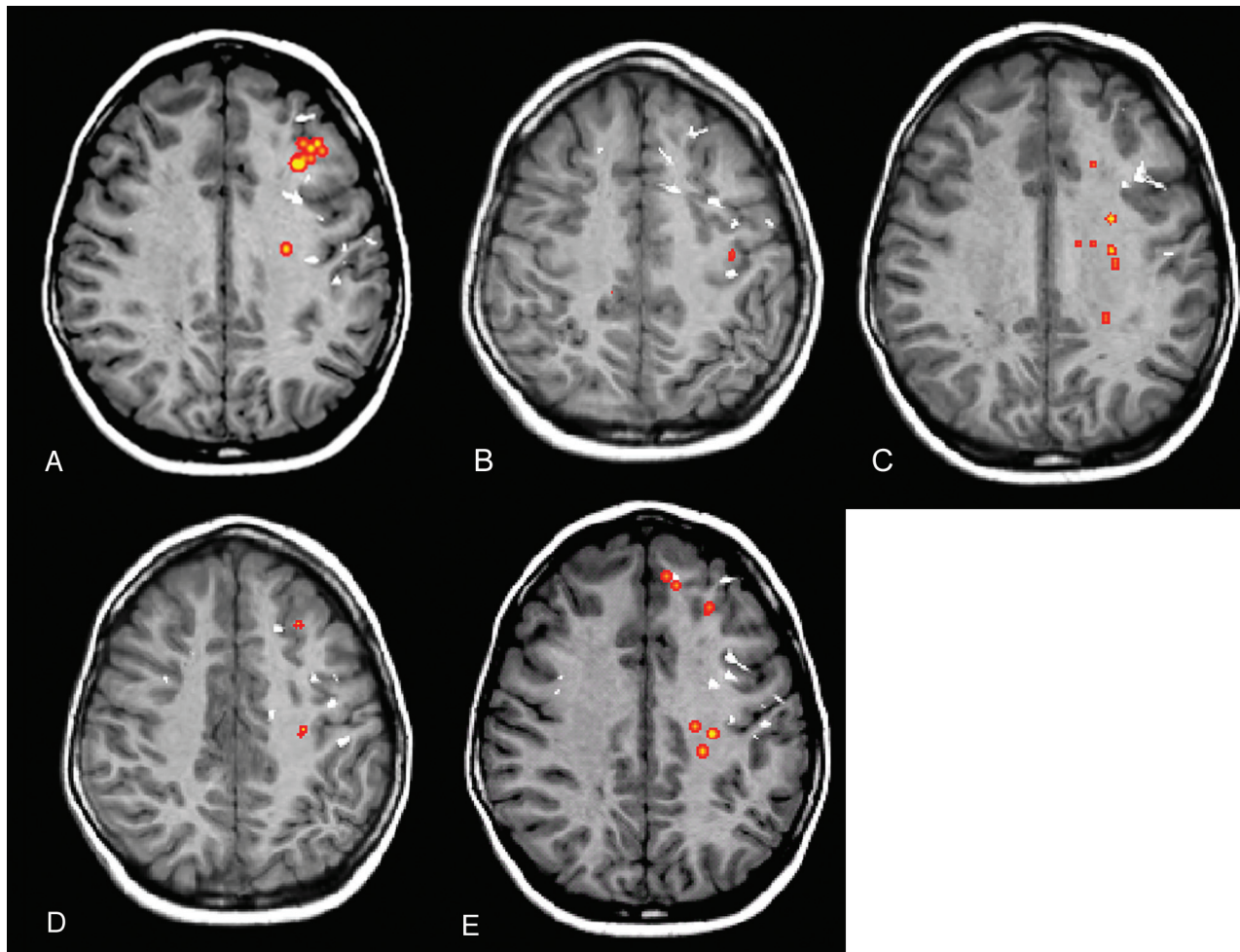
Fig 2. A child with MR imaging-negative epilepsy localized to the left frontal lobe (case 17). Regions with abnormal FA (*A*), MD (*B*), λ_1 (*C*), λ_2 (*D*), and λ_3 (orange areas) (*E*) and MEG dipoles (white) are overlaid onto a volumetric T1-weighted image. The MEG dipole cluster, corresponding to the epileptogenic zone, is localized to the left frontal lobe and a few scattered dipoles in the right frontal lobe. There is lobar concordance of abnormal FA, MD, and eigenvalues with the MEG dipole cluster. There is also overlap between the x-, y-, and z-axes distributions of abnormal FA, MD, and 3 eigenvalues with the MEG dipole cluster.

overlap between λ_3 abnormality and MR imaging-visible FCD in all 3 x-, y-, and z-axes.

MR Imaging-Negative Localization-Related Epilepsy

There was no interobserver variability with respect to the lobar concordance of DTI abnormalities and the MEG dipole cluster.

Abnormal FA was identified in 16/16 (100%) and was lobar-concordant to the MEG dipole cluster in 11/16 (68.8%) (Fig 2). There was no significant difference in lobar congruence of the abnormal FA and the MEG dipole cluster in those with MR imaging-visible FCD and MR imaging-negative localization-related epilepsy ($\chi^2 = 0.80$, $P = .37$). In 9/16 (56.3%), there was overlap between the FA abnormality and the MEG dipole cluster in all 3 x-, y-, and z-axes (Fig 2 and On-line Table 3).

Abnormal MD was identified in 15/16 (93.8%) and was lobar-concordant to the MEG dipole cluster in 11/16 (68.8%), lobar-discordant to the MEG dipole cluster in 4/16 (25%), and negative in 1/16 (6.3%). There was no significant difference in lobar congruence of abnormal MD and the MEG dipole cluster in those with MR imaging-visible FCD and MR imaging-negative localization-related epilepsy ($\chi^2 = 0.09$, $P = .76$). In

10/16 (62.5%), there was overlap between the MD abnormality and the MEG dipole cluster in all 3 x-, y-, and z-axes.

All 16/16 (100%) cases demonstrated abnormalities in all 3 eigenvalues. Lobar concordance with the MEG dipole cluster was present in 8/16 (50.0%) with λ_1 abnormality and in 10/16 (62.5%) with λ_2 and λ_3 abnormalities. There were no significant differences in lobar concordance of abnormal λ_1, λ_2, and λ_3 and the MEG dipole cluster in MR imaging-visible FCD and MR imaging-negative localization-related epilepsy ($\chi^2 = 0.34$, $P = .56$; $\chi^2 = 0.38$, $P = .54$; $\chi^2 = 0.00$, $P = 1.00$ respectively). There were overlaps between λ_1, λ_2, and λ_3 abnormalities with the MEG dipole cluster in all 3 x-, y-, and z-axes in 8/16 (50%) MR imaging-negative localization-related epilepsy cases for all 3 eigenvalues.

Discussion

Previously, a region-of-interest approach has been used to evaluate the subcortical white matter of malformations of cortical development[32] and FCD[33] in children with epilepsy. The region-of-interest approach is restricted to predefined regions and requires a priori definition of the spatial location of FCD. To overcome the limitations of the region-of-interest approach and allow the whole brain to be studied, voxel-based

techniques have been developed. The most commonly used voxel-based technique is SPM,[19] which has its limitations.[26] It is not possible to achieve a perfect alignment of the subject's brain to the common space, which is a requirement for voxel-wise comparison of anatomically different subjects. Smoothing, which is done to reduce residual errors in alignment, can affect the results of VBM analysis, and apparent group differences can appear and disappear with different smoothing extents.[34] These limitations of SPM voxel-based analysis could partly explain the variability in the reported results of DTI SPM voxel-based analysis in patients with MR imaging epilepsy. The concordance in diffusivity and EEG or stereo-EEG varied from 20% to 50% and concordance in anisotropy varied from 3% to 13%.[20-22]

We found that voxel-based analysis by using TBSS yielded better results in localizing the epileptogenic zone compared with previous reports by using VBM analysis. TBSS has several advantages compared with VBM analysis. First, TBSS allows more precise spatial comparability because the data are projected onto a common skeleton rather than requiring precise voxel matching. Second, smoothing is not required in TBSS, thereby reducing partial volume effects and cross-contamination of different tissues. Focke et al[35] evaluated patients with mesial TLE and found that TBSS was more sensitive than SPM and demonstrated more widespread FA and MD abnormalities both in the ipsilateral and contralateral temporal and extratemporal white matter.

Additional factors, other than DTI analysis, could account for the higher concordance of DTI changes with the epileptogenic zone in our study. The patient population in our study was different from those reported by Thivard et al[20] and Rugg-Gunn et al.[21] Our patients included children 6–18 years of age with a shorter duration of epilepsy (mean, 7.4 years) and earlier seizure onset (mean, 4.9 years) compared with those reported by Thivard et al[20] (18–44 years of age; mean duration of epilepsy, 19.3 years; mean age of seizure onset, 11.8 years) and Rugg-Gunn et al[21] (20–53 years of age; mean duration of epilepsy, 21.5 years). The developing white matter in children may be more vulnerable to focal seizure-induced changes, hence a higher concordance between DTI changes and the epileptogenic zone.

Another difference was the seizure type. Most of our patients had FLE, only 2 had TLE, and 1 had frontotemporal epilepsy. Of the 2 patients with TLE in our study, 1 had DTI changes that localized to the temporal lobe and the other did not. TLE accounted for 6/14 patients in the study by Thivard et al[20] and 9/30 patients in the study by Rugg-Gunn et al.[21] Thivard et al[20] found that most TLE cases did not have diffusion abnormalities or that the abnormalities were unrelated to the stereoelectroencephalographic data. The reason for improved seizure localization of extra-TLE by using DTI was not entirely clear but has been attributed to different epileptic networks in extra-TLE compared with TLE.[20] The greater amount of FLE in our cohort could have contributed to the higher concordance of DTI changes with the epileptogenic zone. The improvement in seizure localization in extra-TLE with DTI is particularly advantageous in children because there is a higher incidence of extra-TLE.[36] The capability of DTI to localize the epileptogenic zone in suspected FLE is helpful because seizure lateralization can be difficult clinically and on EEG due to the rapid spread of seizure focus in FLE.[37,38]

Of the 5 DTI indices, MD demonstrated greater lobar concordance and also greater overlap in all 3 x-, y-, and z-axes with the MEG dipole cluster in patients with MR imaging localization-related epilepsy, similar to the findings in previous studies in adults.[20-22] We have found DTI abnormalities occurring both within and also beyond the epileptogenic zone, similar to findings in previous studies.[20-22] The significance of the DTI changes beyond the epileptogenic zone, including the contralateral hemisphere, remains to be elucidated. It is possible that some of these changes are related to the epileptogenic network, which is more extensive than the epileptogenic zone. Different DTI indices did not co-localize to the same region. The possible reasons for this could include underlying neurobiologic injury that is more widespread than the epileptogenic zone, which could have affected different regions of the brain, or possibly selective vulnerability of different components of the white matter to antiepileptic medications.

There are several limitations of our study. We have included subjects with a wide age range, from 5 to 18 years of age. DTI indices are known to change with white matter maturation.[39,40] We have excluded younger children because elevation in FA and reduction in ADC to adult values were found to be most pronounced in the first 2 years of life.[40] We also have age-matched the control group to patients to reduce differences between the 2 groups. Differences in age also introduce variability in head size, and the requirement to normalize the brain to a common space may reduce the accuracy of such analysis. Further technical developments that do not require normalization of the brain to a common space are required to improve the accuracy of DTI detection of white matter abnormalities. We have used the MEG dipole cluster to define the epileptogenic zone rather than the subdural grid because not all patients undergo invasive monitoring. In those who underwent invasive monitoring, the MEG dipole cluster localization of the epileptogenic zone was in agreement with invasive monitoring findings. Despite this finding, those with MR imaging-visible FCD were more likely to achieve seizure freedom compared with those with MR imaging epilepsy. Poorer seizure outcomes in those with MR imaging epilepsy have been attributed to multifocal epileptogenic areas, an extensive epileptogenic area that was not adequately defined before surgery, or incomplete resection.[41]

Conclusions

DTI with TBSS may identify white matter changes in children with both MR imaging-visible FCD and MR imaging-negative localization-related epilepsy, which were concordant with the epileptogenic zone in more than half the patients. Lobar concordance was not significantly different between those with MR imaging-visible FCD and MR imaging-negative localization-related epilepsy. Our results by using DTI TBSS to identify the epileptogenic zone in children with intractable epilepsy are encouraging. However, further technical developments in DTI analysis are required to improve detection of the epileptogenic zone.

References

1. Fisher RS, Stein A, Karis J. **Epilepsy for the neuroradiologist.** *AJNR Am J Neuroradiol* 1997;18:851–63
2. Rastogi S, Lee C, Salamon N. **Neuroimaging in pediatric epilepsy: a multimodality approach.** *Radiographics* 2008;28:1079–95
3. Snead OC 3rd. **Surgical treatment of medically refractory epilepsy in childhood.** *Brain Dev* 2001;23:199–207
4. Bourgeois M, Di Rocco F, Sainte-Rose C. **Lesionectomy in the pediatric age.** *Childs Nerv Syst* 2006;22:931–35
5. Wyllie E. **Surgical treatment of epilepsy in children.** *Pediatr Neurol* 1998;19:179–88
6. Spencer S, Huh L. **Outcomes of epilepsy surgery in adults and children.** *Lancet Neurol* 2008;7:525–37
7. Colombo N, Tassi L, Galli C, et al. **Focal cortical dysplasias: MR imaging, histopathologic, and clinical correlations in surgically treated patients with epilepsy.** *AJNR Am J Neuroradiol* 2003;24:724–33
8. Duncan JS. **Imaging and epilepsy.** *Brain* 1997;120(pt 2):339–77
9. Krsek P, Hajek M, Dezortova M, et al. **(1)H MR spectroscopic imaging in patients with MRI-negative extratemporal epilepsy: correlation with ictal onset zone and histopathology.** *Eur Radiol* 2007;17:2126–35
10. McGonigal A, Bartolomei F, Regis J, et al. **Stereoelectroencephalography in presurgical assessment of MRI-negative epilepsy.** *Brain* 2007;130(pt 12):3169–83
11. Jeha LE, Najm I, Bingaman W, et al. **Surgical outcome and prognostic factors of frontal lobe epilepsy surgery.** *Brain* 2007;130(pt 2):574–84
12. Lee SK, Lee SY, Kim KK, et al. **Surgical outcome and prognostic factors of cryptogenic neocortical epilepsy.** *Ann Neurol* 2005;58:525–32
13. Nobili L, Francione S, Mai R, et al. **Surgical treatment of drug-resistant nocturnal frontal lobe epilepsy.** *Brain* 2007;130(pt 2):561–73
14. Tellez-Zenteno JF, Hernandez Ronquillo L, Moien-Afshari F, et al. **Surgical outcomes in lesional and non-lesional epilepsy: a systematic review and meta-analysis.** *Epilepsy Res* 2010;89:310–18
15. Rugg-Gunn FJ, Eriksson SH, Symms MR, et al. **Diffusion tensor imaging in refractory epilepsy.** *Lancet* 2002;359:1748–51
16. Siegel AM, Jobst BC, Thadani VM, et al. **Medically intractable, localization-related epilepsy with normal MRI: presurgical evaluation and surgical outcome in 43 patients.** *Epilepsia* 2001;42:883–88
17. Theodore WH, Katz D, Kufta C, et al. **Pathology of temporal lobe foci: correlation with CT, MRI, and PET.** *Neurology* 1990;40:797–803
18. Zentner J, Hufnagel A, Wolf HK, et al. **Surgical treatment of temporal lobe epilepsy: clinical, radiological, and histopathological findings in 178 patients.** *J Neurol Neurosurg Psychiatry* 1995;58:666–73
19. Ashburner J, Friston KJ. **Voxel-based morphometry: the methods.** *Neuroimage* 2000;11(6 pt 1):805–21
20. Thivard L, Adam C, Hasboun D, et al. **Interictal diffusion MRI in partial epilepsies explored with intracerebral electrodes.** *Brain* 2006;129(pt 2):375–85
21. Rugg-Gunn FJ, Eriksson SH, Symms MR, et al. **Diffusion tensor imaging of cryptogenic and acquired partial epilepsies.** *Brain* 2001;124(pt 3):627–36
22. Chen Q, Lui S, Li CX, et al. **MRI-negative refractory partial epilepsy: role for diffusion tensor imaging in high field MRI.** *Epilepsy Res* 2008;80:83–89
23. Hermann B, Seidenberg M, Bell B, et al. **The neurodevelopmental impact of childhood-onset temporal lobe epilepsy on brain structure and function.** *Epilepsia* 2002;43:1062–71
24. Symms MR, Barker GJ, Francione F, et al. **Correction of eddy current distortions in diffusion-weighted echo-planar images with a two dimensional registration technique.** In: *Proceedings of the Fifth Scientific Meeting and Exhibition of the International Society for Magnetic Resonance in Medicine*, Vancouver, British Columbia, Canada. April 12–18, 1997:1723
25. Basser PJ, Mattiello J, LeBihan D. **MR diffusion tensor spectroscopy and imaging.** *Biophys J* 1994;66:259–67
26. Smith SM, Jenkinson M, Johansen-Berg H, et al. **Tract-based spatial statistics: voxelwise analysis of multi-subject diffusion data.** *Neuroimage* 2006;31:1487–505
27. Smith SM. **Fast robust automated brain extraction.** *Hum Brain Mapp* 2002;17:143–55
28. Nichols TE, Holmes AP. **Nonparametric permutation tests for functional neuroimaging: a primer with examples.** *Hum Brain Mapp* 2002;15:1–25
29. Holowka SA, Otsubo H, Iida K, et al. **Three-dimensionally reconstructed magnetic source imaging and neuronavigation in pediatric epilepsy: technical note.** *Neurosurgery* 2004;55:1226
30. Iida K, Otsubo H, Mohamed IS, et al. **Characterizing magnetoencephalographic spike sources in children with tuberous sclerosis complex.** *Epilepsia* 2005;46:1510–17
31. Iida K, Otsubo H, Matsumoto Y, et al. **Characterizing magnetic spike sources by using magnetoencephalography-guided neuronavigation in epilepsy surgery in pediatric patients.** *J Neurosurg* 2005;102(2 suppl):187–96
32. Widjaja E, Blaser S, Miller E, et al. **Evaluation of subcortical white matter and deep white matter tracts in malformations of cortical development.** *Epilepsia* 2007;48:1460–69
33. Widjaja E, Zarei Mahmoodabadi S, Otsubo H, et al. **Subcortical alterations in tissue microstructure adjacent to focal cortical dysplasia: detection at diffusion-tensor MR imaging by using magnetoencephalographic dipole cluster localization.** *Radiology* 2009;251:206–15
34. Park HJ, Westin CF, Kubicki M, et al. **White matter hemisphere asymmetries in healthy subjects and in schizophrenia: a diffusion tensor MRI study.** *Neuroimage* 2004;23:213–23
35. Focke NK, Yogarajah M, Bonelli SB, et al. **Voxel-based diffusion tensor imaging in patients with mesial temporal lobe epilepsy and hippocampal sclerosis.** *Neuroimage* 2008;40:728–37
36. Prats AR, Morrison G, Wolf AL. **Focal cortical resections for the treatment of extratemporal epilepsy in children.** *Neurosurg Clin N Am* 1995;6:533–40
37. Harvey AS, Hopkins IJ, Bowe JM, et al. **Frontal lobe epilepsy: clinical seizure characteristics and localization with ictal 99mTc-HMPAO SPECT.** *Neurology* 1993;43:1966–80
38. Talairach J, Tournoux P, Musolino A, et al. **Stereotaxic exploration in frontal epilepsy.** In: Chauvel P, Delgado-Escueta AV, Halgren E, et al, eds. *Frontal Lobe Seizures and Epilepsies*. New York: Raven Press; 1992:651–88
39. Schmithorst VJ, Wilke M, Dardzinski BJ, et al. **Correlation of white matter diffusivity and anisotropy with age during childhood and adolescence: a cross-sectional diffusion-tensor MR imaging study.** *Radiology* 2002;222:212–18
40. Hermoye L, Saint-Martin C, Cosnard G, et al. **Pediatric diffusion tensor imaging: normal database and observation of the white matter maturation in early childhood.** *Neuroimage* 2006;29:493–504
41. Bien CG, Szinay M, Wagner J, et al. **Characteristics and surgical outcomes of patients with refractory magnetic resonance imaging-negative epilepsies.** *Arch Neurol* 2009;66:1491–99